Construction and Building Materials 118 (2016) 116–126

Contents lists available at ScienceDirect

Construction and Building Materials

journal homepage: www.elsevier.com/locate/conbuildmat

Size effect on axial stress-strain behavior of CFRP-confined square concrete columns

D.Y. Wang [a,b], Z.Y. Wang [a,b,*], S.T. Smith [c], T. Yu [d]

[a] Key Lab of Structures Dynamic Behavior and Control of the Ministry of Education, Harbin Institute of Technology, Harbin, China
[b] School of Civil Engineering, Harbin Institute of Technology, Harbin, China
[c] School of Environment, Science and Engineering, Southern Cross University, Lismore, NSW 2480, Australia
[d] Faculty of Engineering and Information Sciences, University of Wollongong, Wollongong, NSW, Australia

HIGHLIGHTS

- Axial stress-strain behavior of FRP-confined square concrete columns.
- Influence of size effect on column behavior and FRP effective strain.
- Experimental investigation and model development for FRP-confined concrete columns.
- Calibration of effective strain model considering size in FRP-confined columns.

ARTICLE INFO

Article history:
Received 6 January 2016
Received in revised form 19 April 2016
Accepted 27 April 2016
Available online 12 May 2016

Keywords:
FRP
Confined concrete
Square column
Size effect
Stress-strain behavior

ABSTRACT

Research published on the axial compressive behavior of fibre-reinforced polymer (FRP)-confined concrete columns has been generally based on small-sized specimens. There have been limited studies published on large-sized columns and there have also been limited studies on the validity of upscaling results obtained from small-sized specimens. On account of such knowledge gap, this paper presents the test results of 23 carbon FRP-confined square concrete columns of varying sizes subjected to monotonic axial compression. The specimens were sorted into 10 groups based on (i) specimen size, (ii) theoretical lateral FRP confining pressure, (iii) number of layers of FRP wrap, and (iv) inclusion and exclusion of internal steel reinforcement. In each group, the specimens consisted of different cross-sectional sizes but the same theoretical lateral confining pressure. The experimental results showed that specimen size had no significant effect on the axial stress-strain behavior of FRP-confined medium- and small-sized columns (i.e. sections defined herein equal to and less than 300 mm in width). The axial stress-strain responses exhibited differences as the specimen size increased. This was especially the case for FRP-confined large-sized columns (i.e. sections defined herein equal to and larger than 350 mm in width). The rupture strain of the FRP wrap at the corner regions is proposed to be defined as the effective lateral rupture strain of FRP, and this strain was shown to decrease with an increase of specimen size. Based on the test results, a modified FRP effective strain factor model considering the influence of size effect is proposed.

1. Introduction

The axial compressive behavior of fibre-reinforced polymer (FRP)-confined concrete has received significant attention over the last two decades. As a result, it is now well established that the confinement of concrete with FRP composites can substantially enhance concrete strength and ductility. A number of experimental and theoretical investigations have been conducted to date on FRP-confined concrete columns [1–13]. The majority of such studies have focused on the axial compressive performance of FRP-confined small-sized cylinders and prisms. In cases, axial stress-strain models have been developed and such models are very important for the design of FRP-strengthened structures. Small specimens, as opposed to large-sized specimens, are widely used in tests since they are relatively easy to handle, economical, and typically require more readily available test equipment of lesser size and capacity. However, the validity of extrapolating results

* Corresponding author at: Room 520, School of Civil Engineering, Harbin Institute of Technology, Harbin, 150090, China.
E-mail addresses: daiyuwang@hit.edu.cn (D.Y. Wang), zhenyuwang@hit.edu.cn (Z.Y. Wang), scott.smith@scu.edu.au (S.T. Smith), taoy@uow.edu.au (T. Yu).

http://dx.doi.org/10.1016/j.conbuildmat.2016.04.158
0950-0618/

from small-sized test specimens as well as the proposed models arising to more realistic larger-sized columns has been largely devoid of research. Moreover, design codes for concrete structures retrofitted with FRP composites [14,15] do not consider size effect. In this paper, large-size, medium-size, small-size and very small-size columns are defined by cross-sectional dimensions of about 350 mm (and greater), 250 mm, 100 mm, and 50 mm, respectively. These sizes are based on comparison with real structures by the authors and they have also been defined in a similar manner in other studies as well [16–18].

Limited studies have been conducted on the influence of cross-sectional size on the axial compressive behavior of FRP-confined concrete columns [16–25]. For FRP-confined circular columns, most of the existing studies indicated that the cross-sectional size has no obvious influence on the axial stress-strain behavior. For example, Thériault et al. [16] tested FRP-confined circular columns with three different diameters and two different slenderness ratios. The test results indicated that no significant size effect was observed for medium-(152 mm in diameter) and large-sized (304 mm in diameter) columns. Size effects were evident only in very small specimens of 51 mm in diameter. Carey and Harries [19] investigated the axial behavior of FRP-confined circular columns with similar confining stiffness but different sizes. The results showed that the column sizes had no significant influence on the axial stress-strain behavior. Zhu et al.'s [20] experimental studies on the axial compression behavior of concrete-filled FRP tubes showed that specimen size did not appear to influence either the confinement or the overall axial compression response. In another study, Elsanadedy et al. [17] investigated experimentally and numerically the influence of size effect on FRP-wrapped concrete circular columns. Thirty-seven concrete cylinders with three different sizes (50, 100 and 150 mm in diameter) were tested. The test and numerical results showed the effect of specimen size on FRP-confined circular concrete columns to be insignificant. Nevertheless, Pessiki et al. [21] indicated that the stiffness of the FRP confinement in specimens of small-size may be significantly greater than larger-sized columns that would be expected in practice. Cross-section geometry therefore significantly influenced the axial behavior of FRP jacketed specimens.

Studies on FRP-confined noncircular columns, however, produced results opposite to circular columns in that the cross-sectional size significantly influenced the axial compressive behavior. For example, Masia et al. [22] tested the axial compressive behavior of 30 square columns with 3 different cross-sectional sizes (100 mm, 125 mm and 150 mm). The test results indicated that the effectiveness of the FRP confinement reduced with increasing cross-sectional size. However, in this study the corner radius was 25 mm for all the specimens. In this case, the shape factor of small-sized columns was larger than that of larger-sized columns. Note that the shape factor refers to the ratio of the effectively confined concrete to the total cross-sectional area of concrete. Consequently, the results in this study were influenced not only by cross-sectional size but also the corner radius (r_c). The conclusions of the influence of size effect are therefore questionable. Rocca [23] tested larger-sized FRP-confined square RC columns with cross-sectional widths (b) of 324 mm, 457 mm, 648 mm and 914 mm. The test results showed clear differences in the axial stress-strain behavior between smaller and larger columns. Toutanji et al. [18] tested three field-size square (355 × 355 mm) and rectangular (250 × 500 mm) columns under axial compression. Based on test results, existing ultimate axial strength and stress-strain models which have mostly been developed for small-scale specimens were evaluated. The comparison indicated that some models failed to adequately characterize the axial stress-strain response of the tested large-scale columns. Wang and Wu [24] studied experimentally the size effect of short concrete columns confined with aramid FRP (AFRP). The test results demonstrated that specimen size had significant effect on the strength of confined columns, but it had lesser effect on the axial stress-strain curves. It also had a slight effect on the failure modes. Based on the test results, a sized-dependent stress model was proposed by modifying Bažant's size-effect law. Finally, Wang et al. [25] investigated the axial stress-strain behavior of carbon FRP (CFRP)-confined larger-sized concrete square columns with two specimen sizes but the same ratio of r_c/b. Their test results showed that the effective lateral confinement of CFRP was significantly influenced by the cross-sectional dimensions of the confined columns. In summary, existing studies have mostly confirmed that cross-sectional size has no real apparent influence on the behavior of FRP-confined circular columns, but it does have significant effect on FRP-confined noncircular columns. As findings to date are not that conclusive, further research on the influence of size effect on FRP-confined noncircular columns is warranted.

This paper presents an experimental study on CFRP-confined square columns with different cross-sectional sizes subjected to monotonic axial compression. A total of 23 unreinforced and reinforced concrete columns divided into 10 groups were fabricated and tested. Five of the groups consisted of plain concrete columns while the other five groups consisted of concrete columns reinforced with steel reinforcement. In each group, the specimens consisted of different cross-sectional sizes but the same theoretical lateral confining pressure calculated according to ACI 440.2R-08 [14]. The test results are used to confirm whether size effect exists in FRP-confined square columns, especially in larger-sized columns. A new FRP effective strain factor model for FRP-confined square concrete columns, considering the influence of cross-sectional size, is finally proposed.

2. Experimental program

2.1. Test specimens and materials

The test specimens consisted of seven different cross-sectional sizes which varied from 100 mm to 400 mm, as shown in Fig. 1. All specimens, however, contained the same height to cross-sectional width ratio (H/b) of 3.0 in order to ensure the influence of slenderness ratio was not a test variable. Existing studies have demonstrated that the confinement efficiency of wrapped FRP was significantly influenced by the corner radii of noncircular columns [26]. However, on account of the position of the internal steel reinforcement, the corner radius cannot be rounded as large as ideally desired. To ensure the influence of corner radius was the same for all the specimens, the corner radius to width ratio (r_c/b) was set to be constant value of 0.15 for all specimens. The test specimens were divided into 10 groups. Five of the groups (i.e. groups GA1 to GA5) consisted of plain concrete columns while the remaining five groups (i.e. groups GB1 to GB5) consisted of concrete columns reinforced with steel reinforcing bars. The specimens of each group contained different cross-sectional sizes but the same theoretical lateral FRP confining pressure according to ACI 440.2R-08 [14]. For the steel reinforced specimens, approximately the same longitudinal and lateral steel reinforcement ratios were maintained.

The lateral FRP confining pressure model adopted by ACI 440.2R-08 [14] is expressed as:

$$f_l = \frac{2E_f n t_f \varepsilon_{fe}}{D} \quad (1)$$

where f_l = lateral confining pressure of FRP, E_f = elastic modulus of FRP, n = number of layers of fibre sheet, t_f = thickness of one ply of FRP wrap, ε_{fe} = effective lateral strain of FRP at failure, and D = diameter of circular column. For noncircular cross sections, f_l in Eq. (1) corresponds to the lateral confining pressure of an equivalent circular cross section with diameter D equal to the length of the diagonal of a rectangular cross section as follows

$$D = \sqrt{b^2 + h^2} \quad (2)$$

where b = section width and h = depth of column section. As a result, the equivalent diameter of square columns is equal to $[\sqrt{2}b$. For the reinforced concrete columns investigated, the longitudinal steel reinforcement ratio and the volumetric ratio of the hoop reinforcement were approximately equal to 1.5% and 0.4%, respectively. In addition, the hoop reinforcements were terminated inside the core concrete using a 90° hook in order to simulate non-ductile RC columns. The reinforcement details of each group are illustrated in Fig. 1.

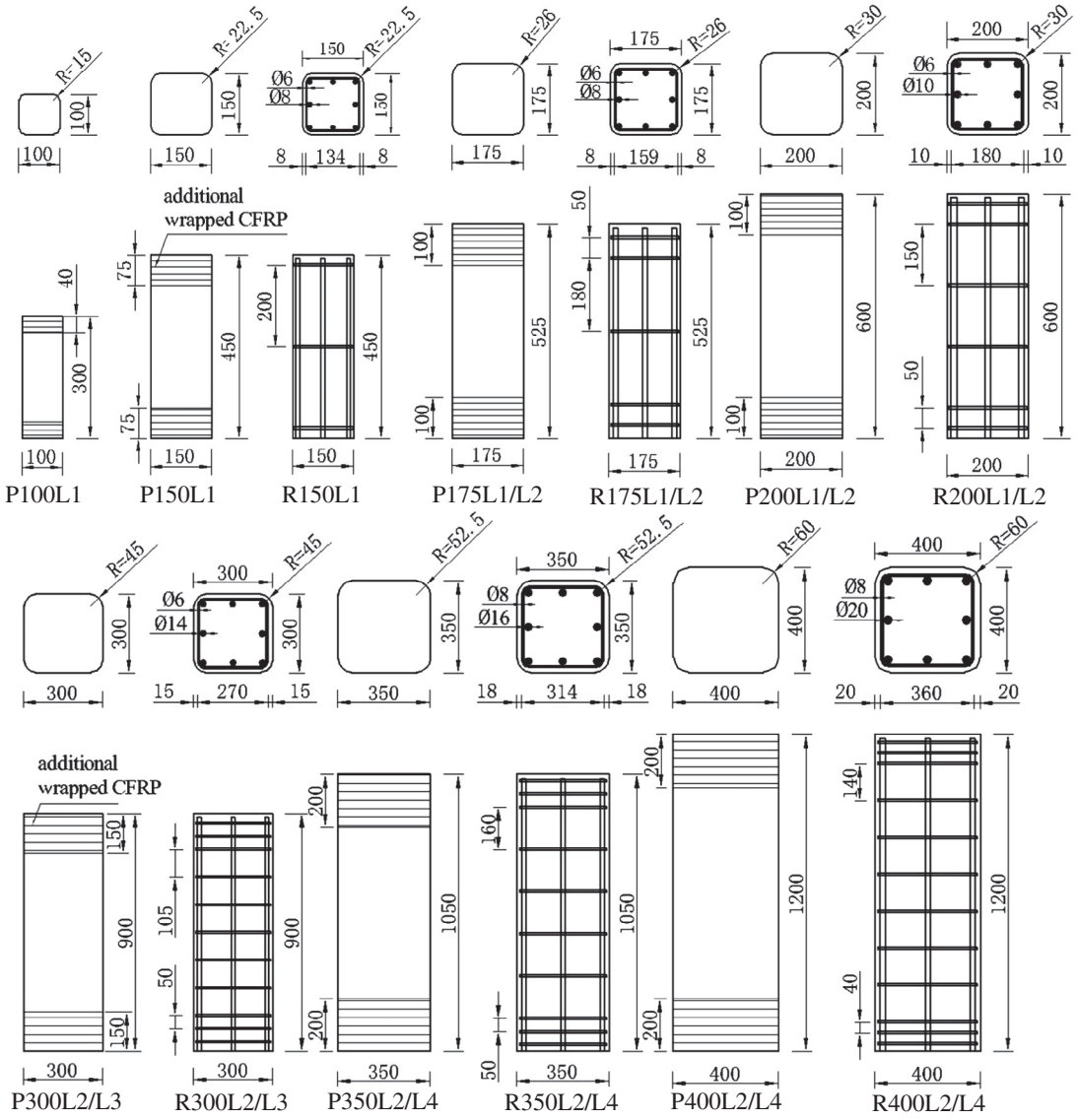

Fig. 1. Specimen dimensions and reinforcement details.

The columns were produced from one batch of ready mixed concrete that was poured into wooden molds. Each corner radius (r_c) of each mold was defined by inserting quarter circular shaped iron sheets. The average compressive cylinder strength during column tests was 25.4 MPa. After the concrete had achieved an age of 28 days, a high tensile strength uni-directional carbon fibre sheet was applied in the hoop direction in a wet lay-up manner for the required number of layers of each wrapped specimen. In order to avoid premature failure, intervention strategies were implemented. These strategies consisted of adding internal hoop reinforcement spaced at 50 mm centers at the column ends, and adding one additional layer of CFRP wrap extending from 40 mm to 200 mm for column widths varying from 100 mm to 400 mm, respectively. The material properties of the CFRP were obtained by testing six flat coupons of 25 mm width and 200 mm length in accordance with ASTM D3039 [27]. In addition, the properties of the steel reinforcement were determined in accordance with ASTM E8/E8M [28]. Table 1 provides a summary of the FRP and steel test results.

Table 2 provides a comprehensive overview of the details of the test specimens. The specimen identification convention utilized in Table 2 is based on the first letter P or R referring to unreinforced (plain) or reinforced concrete, respectively. The following number in the specimen identification refers to the cross-sectional size (e.g. 100 = 100 mm wide section). The last letter L and number following refer to the number of layers of carbon fibre sheet wrap.

Table 1
Tested mechanical properties of steel reinforcement and CFRP wrap.

Material	Diameter/ thickness (mm)	Yield strength (MPa)/rupture strain	Ultimate strength (MPa)	Elastic modulus (GPa)
Longitudinal steel	$d_s = 8$	$f_y = 418$	$f_{su} = 502$	$E_s = 210$
	$d_s = 10$	$f_y = 356$	$f_{su} = 515$	$E_s = 210$
	$d_s = 14$	$f_y = 380$	$f_{su} = 480$	$E_s = 210$
	$d_s = 16$	$f_y = 350$	$f_{su} = 446$	$E_s = 210$
	$d_s = 20$	$f_y = 328$	$f_{su} = 466$	$E_s = 210$
Hoop steel	$d_s = 6$	$f_y = 338$	$f_{su} = 479$	$E_s = 200$
CFRP	$t_f = 0.167$	$\varepsilon_{fe} = 0.18\%$	$f_f = 4340$	$E_f = 240$

2.2. Instrumentation and testing

The test setup and instrumentation layout are shown in Fig. 2. All of the column tests were conducted in an Amsler universal test machine of 5000 kN capacity. In addition, the applied load was measured via a load cell installed at the top of each test column. The CFRP and steel reinforcement strains were measured using strain gauges of gauge lengths 10 mm and 2 mm, respectively. Wang et al.'s [25] tests indicated that the effective strain could be based on the hoop strains at the corner regions of the column section. Consequently, in this study more attention was paid to instrumentation of the corner regions. Strain gauges were therefore adhered to the surface of the CFRP wrap in the hoop direction at column mid-height to measure hoop strain while extra strain gauges were mounted at the corner regions, as shown in Fig. 2. For all column tests, the axial strains were calculated from four longitudinally oriented linear variable differential transformers (LVDTs). These LVDTs were fixed on the columns by two steel frames as shown in Fig. 2. The LVDTs were located at the four corner regions of each specimen with the gauge length being equal to about one third of the column height. For RC columns, strain gauges

Table 2
Specimen details and summary of test results.

Specimen		b mm	H mm	r_c mm	LRB	Hoops	n	f_l MPa	f_{c0} MPa	$\frac{f_{cu}}{f_{c0}}$	ε_{cu} %	$\varepsilon_{h,rup}$ %	$\varepsilon_{m,rup}$ %	ε_{fe} %
GA1	P100L1	100	300	10	–	–	1	6.01	25.7	1.56	2.280	−1.114	−1.208	−1.083
	P200L2	200	600	28	–	–	2	6.01	24.6	1.53	1.934	−0.897	−0.969	−0.849
	P300L3	300	900	42	–	–	3	6.01	22.7	1.55	2.824	−0.751	−0.781	−0.729
	P400L4	400	1200	45	–	–	4	6.01	21.1	1.27	1.884	−0.615	−0.729	−0.501
GA2	P150L1	150	450	20	–	–	1	4.00	25.4	1.48	2.229	−1.087	−1.403	−0.993
	P300L2	300	900	35	–	–	2	4.00	22.7	1.43	1.837	−0.794	−0.928	−0.700
GA3	P175L1	175	525	25	–	–	1	3.43	25.2	1.39	1.738	−1.121	−1.155	−1.020
	P350L2	350	1050	45	–	–	2	3.43	21.9	1.22	1.141	−0.711	−0.815	−0.617
GA4	P175L2	175	525	25	–	–	2	6.86	25.2	1.77	2.333	−0.897	−0.898	−0.897
	P350L4	350	1050	40	–	–	4	6.86	21.9	1.51	2.807	−0.768	−0.904	−0.660
GA5	P200L1	200	600	25	–	–	1	3.00	24.6	1.21	1.112	−0.917	−1.017	−0.797
	P400L2	400	1200	55	–	–	2	3.00	21.1	1.03	1.434	−0.638	−0.728	−0.587
GB1	R200L2	200	600	23	8ϕ10	ϕ6@160	2	6.01	24.6	1.71	2.200	−0.897	−1.153	−0.743
	R300L3	300	900	42	8ϕ14	ϕ6@105	3	6.01	22.7	1.75	2.954	−0.853	−1.009	−0.715
	R400L4	400	1200	52	8ϕ20	ϕ8@140	4	6.01	21.1	(1.13)	(0.591)	(−0.139)	(−0.149)	(−0.099)
GB2	R150L1	150	450	19	8ϕ8	ϕ6@200	1	4.00	25.4	1.25	1.115	−0.864	−0.969	−0.866
	R300L2	300	900	45	8ϕ14	ϕ6@105	2	4.00	22.7	1.50	2.012	−0.804	−0.977	−0.696
GB3	R175L1	175	525	26	8ϕ8	ϕ6@180	1	3.43	25.2	1.53	1.253	−0.967	−0.993	−0.949
	R350L2	350	1050	48	8ϕ16	ϕ8@160	2	3.43	21.9	1.19	0.924	−0.532	−0.539	−0.528
GB4	R175L2	175	525	24	8ϕ8	ϕ6@180	2	6.86	25.2	2.21	2.343	−0.953	−0.996	−0.934
	R350L4	350	1050	45	8ϕ16	ϕ8@160	4	6.86	21.9	(1.49)	(0.923)	(−0.409)	−(0.421)	(−0.399)
GB5	R200L1	200	600	27	8ϕ10	ϕ6@160	1	3.00	24.6	1.33	1.011	−0.745	−0.752	−0.730
	R400L2	400	1200	58	8ϕ20	ϕ8@140	2	3.00	21.1	(1.13)	(0.355)	(−0.165)	(−0.170)	(−0.161)

Note: The axial stress and strain are defined as positive and the lateral strain as negative; P = plain concrete; R = reinforced concrete; b = nominal width of cross section; H = nominal height of specimen; r_c = measured corner radius; LRB = longitudinal reinforcement bars; n = layers of wrapped CFRP; f_l = theoretical lateral FRP confining pressure; f_{c0} = peak stress of unreinforced concrete columns considering size effect; f_{cu} = ultimate stress of confined concrete at failure; ε_{cu} = strain corresponding to f_{cu}; $\varepsilon_{h,rup}$ = average lateral rupture strain of all CFRP strain gauges; $\varepsilon_{m,rup}$ = average lateral rupture strain of CFRP strain gauges at middle of sides; ε_{fe} = average lateral rupture strain of CFRP strain gauges at corners. Note that values in brackets refer to maximum recorded result (i.e. not based on failure of test specimen).

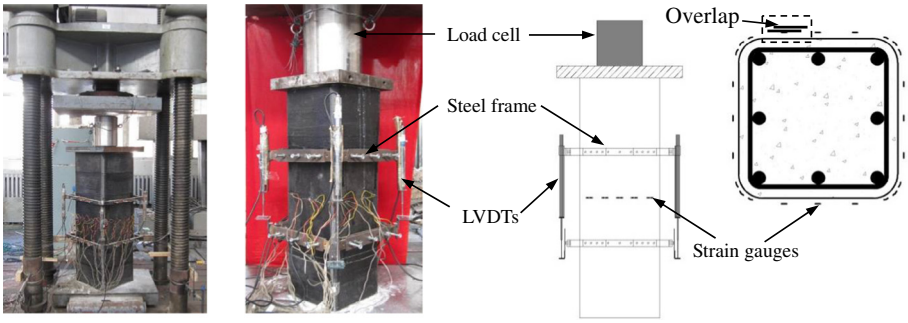

Fig. 2. Test setup and instrumentation details.

were bonded onto the hoop and longitudinal steel reinforcement to measure the strain of the internal reinforcement.Before testing, the specimens were pre-loaded/unloaded to 0.2 $f_{c0}A_g$ in order to center the load (note that A_g is the gross section of each specimen). During the preload/unload process, the position of specimens were adjusted until the monitored values of four LVDTs surrounding each specimen were approximately the same. In this case, the specimens were regarded to be subjected to concentric axial load. Then the specimens were initially tested under a load controlled manner at a loading rate of approximately 0.15 MPa/s before the axial load reached the compressive concrete cylinder strength. After the compressive cylinder concrete strength was reached, the load was then applied in a constant displacement control manner at a rate of approximately 0.00004 mm/mm/s.

3. Test results and discussion

3.1. Failure modes

The test specimens failed suddenly due to rupture of the CFRP wraps and this failure mode is consistent with observations arising from previous studies on FRP-confined square columns [25]. On the whole, the specimen size appeared to have no obvious influence on the failure mode. Generally, the CFRP rupture originated near the corner regions within the mid-height of the test columns as shown in Fig. 3. The treatments applied to the column ends were successful in ensuring failure in the mid-height region of the columns. Following removal of the CFRP wraps post-test, it was evident that the columns experienced diagonal failure surfaces with severe concrete crushing. In addition, for the columns reinforced with internal steel, the internal hoop reinforcement bent outward and the longitudinal bars buckled as also shown in Fig. 3.

3.2. Axial stress-strain responses

Previous studies have verified a notable size effect on the nominal strength of plain concrete [29–33] and a widely recognized model is Bažant's size-effect law [29]. Considering the energy balance at crack propagation in concrete, the model was derived from

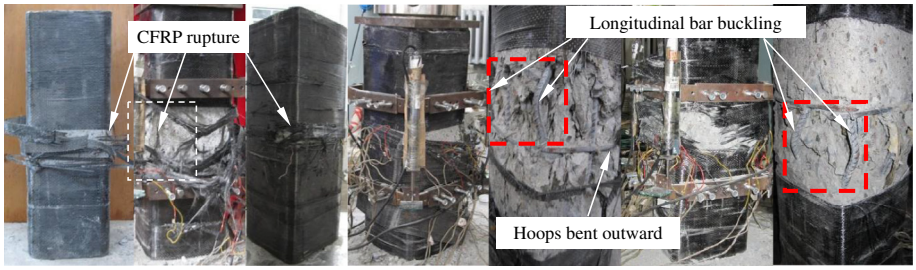

Fig. 3. Typical failure mode.

a dimensional analysis for geometrically similar concrete members. The model is given as follows:

$$\sigma_N = \frac{P}{bd} = \frac{Bf'_t}{\sqrt{1+\frac{d}{\lambda_0 d_a}}} \tag{3}$$

where σ_N = nominal stress; P = maximum load; b = thickness (mm); d = characteristic dimension (mm); f'_t = direct tensile strength of concrete; d_a = maximum aggregate size, and B and λ_0 are empirical constants. Consequently, the compressive strength of unconfined concrete columns with different size should be different due to the size effect. For the uniaxial compression strength, substituting f'_t for the standard cylinder compression strength f'_c, Bažant [30], Kim et al. [32], and Zhou [33] proposed the modified size effect model for the compressive strength of concrete. The compressive cylinder strengths (f_{c0}) corresponding to specimens tested herein with different cross-sectional diameters were calculated using the existing modified models. The standard cylinder compression strength (i.e. 25.4 MPa) was used to verify the prediction accuracy of these models. It was found that the modified model proposed by Zhou predicted the most accurate results. Consequently, the Zhou's model was finally adopted to calculate compressive cylinder strengths corresponding to each specimen, as shown in Table 2. The empirical constants of B and $\lambda_0 d_a$ in the final adopted model were equal to 1.207 and 364.1, respectively. To eliminate size effect on the compressive strength of unconfined columns, the experimental axial stress of each specimen was normalized by dividing by the corresponding value of f_{c0}. The normalized results in each group were then compared to verify whether column size influenced the effective lateral confinement of FRP in addition to the stress-strain behavior of FRP-confined columns.

The normalized experimental axial stress-strain curves of each group are presented in Fig. 4 and a summary of key test results of all specimens is provided in Table 2. In Fig. 4 and Table 2, the axial stress and strain are defined as positive and the lateral strain as negative. Axial stress was obtained from dividing the axial load by the entire cross-sectional area of concrete, while the contribution of longitudinal steel reinforcement was deducted considering the axial stress-strain relationship of steel bars for the RC columns. The axial strain was derived from the average of the four LVDTs, mounted onto each test specimen, divided by their gauge length. In this table, the ultimate axial stress f_{cu} and the corresponding strain ε_{cu} are equal to the stress and strain at failure, respectively. For hoop strain, the average lateral rupture strain of all the mounted strain gauges on the CFRP wraps is $\varepsilon_{h,rup}$, while ε_{fe} and $\varepsilon_{m,rup}$ refer to the average lateral rupture strain of the strain gauges mounted at the corner regions and middle regions of each side, respectively. It can be noted that specimens R350L4, R400L2, and R400L4 were not tested to failure as the load bearing capacity of these columns exceeded the load capacity of the test machine. These three columns were finally loaded to approximately 4850 kN. Therefore, the stress and strain of these 3 columns shown in Table 2 are based on the maximum applied load, and not the load at failure. These results are enclosed in brackets in this table.

It can be seen from Table 2 and Fig. 4 that no obvious differences in the stress-strain responses can be observed in each group for cross-sectional sizes equal to and less than 300 mm in width. However, the normalized stress-strain curves of large-sized specimens (cross-section larger than 300 mm) exhibit significant differences compared with the smaller columns under the same theoretical lateral FRP confining pressure. This is especially the case for stress capacity. For example, the normalized ultimate stresses of P100L1, P200L2 and P300L3 in group GA1 are all approximately equal to 1.55. This value reduces to 1.27 as the specimen size increases to 400 mm (P400L4) while the ultimate strain capacity also slightly decreases. In group GA2, the entire normalized stress-strain curves of P150L1 and P300L2 are approximately the same. Similar results are also observed in FRP-confined RC columns (i.e. GB1). Moreover, the trend of the stress-strain curves varies if the number of layers of wrap is insufficient (i.e. in GA5 the stress-strain curve of P200L1 exhibits a monotonic ascending branch, while for specimen P400L2 the stress-strain curve exhibits a final descending response). In addition, the differences of stress-strain behavior between large and small columns are more obvious in FRP-confined RC columns. For example, the normalized ultimate stress of P175L1 and P350L2 (GA3) is 1.39 and 1.22, respectively. The reduction in stress capacity with an increase of column size is approximately 12% for these FRP-confined unreinforced columns. However, for FRP-confined RC columns with the same size and lateral confinement (i.e. GB3) the normalized ultimate stress is decreased from 1.53 (R175L1) to 1.19 (R350L2) and the second portion of stress-strain curve is also changed from the ascending branch to approximately a horizontal line. The reduction is up to about 22% with the existence of internal steel reinforcement.

Fig. 5 presents a comparison of the normalized ultimate stress of FRP-confined unreinforced concrete and RC columns. The results have been grouped according to uniform cross section size and number of layers of CFRP wrap. It can be observed that the ultimate stresses of the RC columns are usually larger than those of the unreinforced concrete columns. As the volumetric ratios of the hoop reinforcement for all the RC columns is only 0.4%, the lateral confinement pressure arising is small. Consequently, the enhancement in peak stress of the concrete resulting from hoop steel confinement is very limited. The increment is only about 6% based on the stress-strain model of reinforced concrete as proposed by Scott et al. [34]. In this case, the normalized ultimate stress of confined RC columns minus the contribution of hoop reinforcement is still larger than that of the unreinforced columns. For example, the normalized ultimate stress of R200L2 and R300L3 after subtraction of the contribution of hoop steel is still no less than 1.65. The values for P200L2 and P300L3 are about 1.55. However, the presence of internal steel bars also may result in premature failure of the confined columns followed by a reduction of stress capacity of the columns. This is due to early buckling of the longitudinal bars and

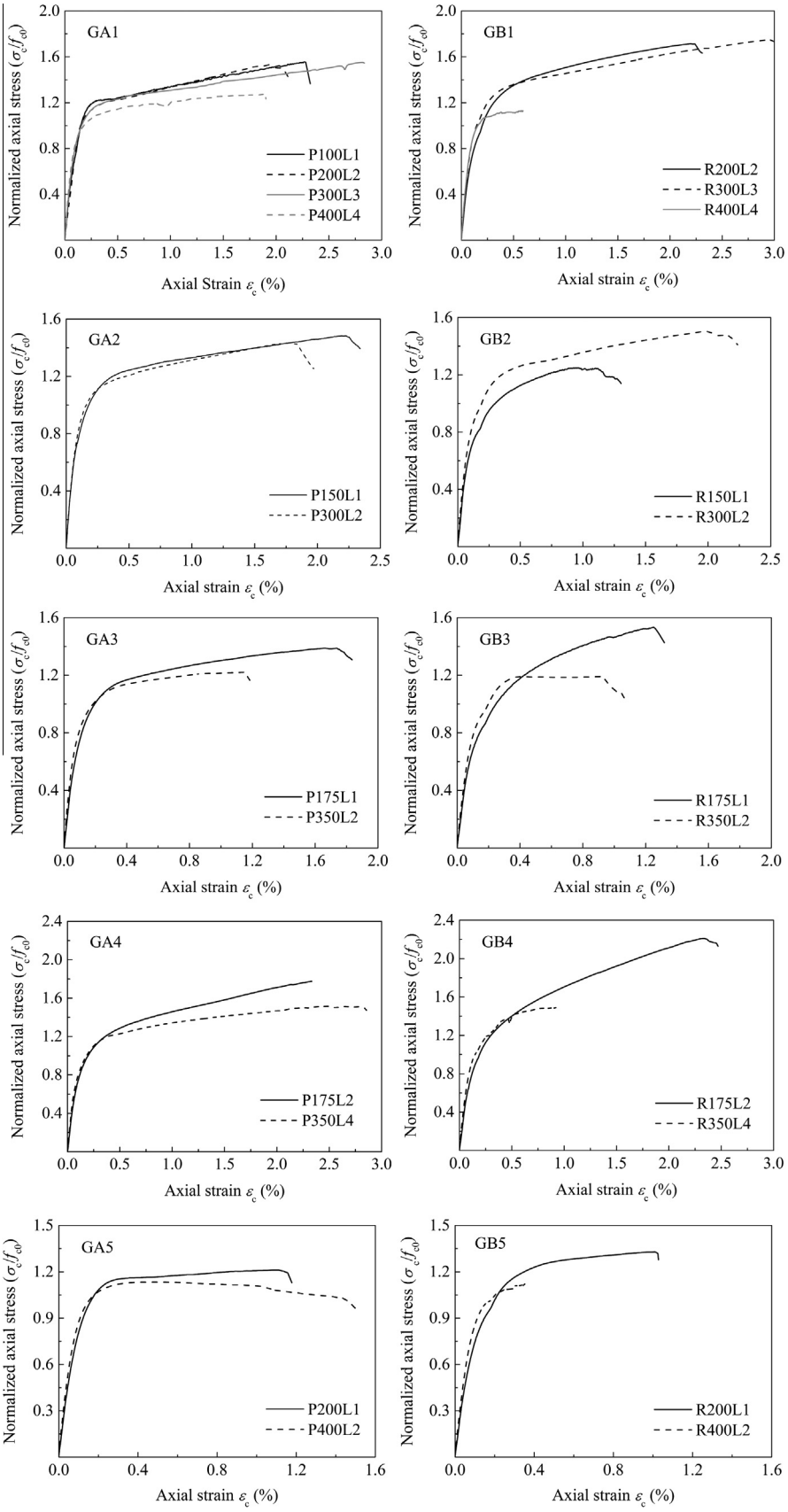

Fig. 4. Normalized experimental axial stress-strain curves of each test group.

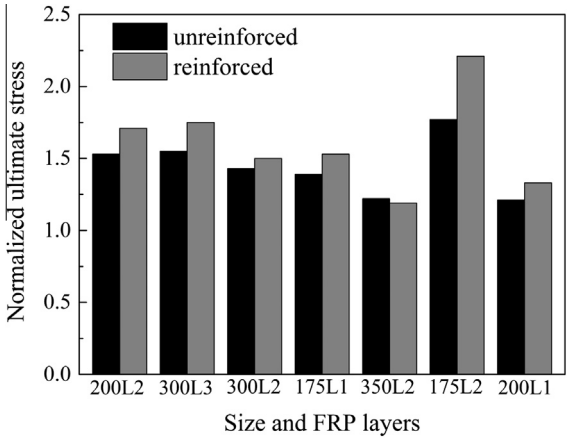

Fig. 5. Normalized ultimate stress of confined unreinforced and reinforced columns.

outside bending of the hoop reinforcement in lightly-confined columns that will result in premature rupture of the FRP. This will further reduce the stress capacity of confined columns. For example, the ultimate stress of R350L2 is less than that of P350L2. This means that the measured FRP rupture strain of the former is less than that of the latter, as shown in Table 2.

From the above discussion it can be concluded that approximately no size effect exists on the axial stress-strain curves of FRP-confined small sized columns (i.e. cross-sectional size equal to and less than 300 mm) after considering the column size on the axial strength of unconfined concrete. The axial stress-strain response exhibits obvious difference with the increase of specimen size, especially for FRP-confined large-size columns (i.e. cross-sectional size larger than 350 mm). The difference of axial compressive behavior between FRP-confined small and large-sized columns is caused mainly by the decrease of lateral confinement of CFRP (more detailed discussions are provided in the next section). This means that the actual confinement provided by CFRP wraps is not the same in each group. The existing stress-strain models that have been based on the test results of smaller columns are therefore not suitable for larger sized columns.

3.3. Hoop strain of CFRP wraps

For FRP-confined columns, the lateral confinement by the FRP wraps is classed as a passive-confinement as the lateral confining pressure increases only upon dilation of the concrete core. Due to the radial displacement compatibility between the concrete and the FRP wrap, the hoop strain of these two parts is considered to be equivalent. As a result, the hoop strain of CFRP wraps can be discussed in greater detail to understand the variation of lateral confinement around the perimeter of the cross-section, as well as the axial stress-strain behavior for FRP-confined columns.

Fig. 6 shows the relationships between axial strain and hoop strain for all strain gauges for four specimens selected from two groups (i.e. P175L2 and P350L4 in GA4, and R150L1 and R300L2 in GB2). The four specimens are selected for several reasons, namely, (1) most of the strain gauges on each specimen remained intact on each specimen for the entire test duration, (2) inclusion of both FRP-confined plain concrete columns (i.e. GA4) and confined RC columns (i.e. GB2), (3) the theoretical lateral confining pressure of CFRP wrap is different between the two groups. It can be seen from Fig. 6 that the increase of CFRP hoop strain at the middle regions are larger than that at the corner regions. In addition, the hoop strains are also larger in the middle regions compared to the corner regions at failure. On account of the differences in hoop strains, the strains at ultimate vary; however, all strains are less than the ultimate tensile strain of flat coupons which is approximately equal to 1.8%. For example for specimen P175L2, the measured rupture strains of all the strain gauges mounted at the corner regions vary from about −0.4% to −0.8% while the values at the middle of the sides vary from −0.8% to −1.6%. Similar results are observed for the tested FRP-confined RC columns (i.e. R300L2).

Table 2 and Fig. 6 show similar results. Here, the ratio of the measured average rupture strain at the corner regions to the ultimate tensile strain of CFRP is smaller than that at middle regions. The ratios are all less than 1.0. For example, the average values of the measured rupture strain of (i) all the mounted strain gauges ($\varepsilon_{h,rup}$), (ii) strain gauges at corner regions (ε_{fe}), and (iii) strain gauges at the middle of the sides ($\varepsilon_{m,rup}$), to the ultimate tensile strain of CFRP from flat coupon test (ε_{fu}) were 0.346, 0.282, and 0.410, respectively, for specimen P400L4. The results provided in Table 2 also indicate that the average value of rupture strain both at the corner and middle regions were all decreased with an increase of cross-sectional size. For example, the ratio of the average measured rupture strain of the strain gauges mounted at the corner regions to the ultimate tensile capacity of CFRP were 0.609, 0.477, 0.410, and 0.282, for specimens P100L1, P200L2, P300L3 and P400L4 in group GA1, respectively.

To better illustrate the distribution of CFRP hoop strain around the entire perimeter of confined columns, Fig. 7 shows the hoop strain at different positions. In this figure the vertical axis represents lateral strain while the horizontal axis represents the position of the strain gauges around the perimeter of the section. It can be observed that the distribution of hoop strain was relatively uniform at low load levels, but there were small variations at different locations. With the axial stress increasing approximately equal to or larger than the peak strength of unconfined concrete (i.e. compressive cylinder strength of 25.4 MPa), quite large variation in CFRP hoop strain at different locations is exhibited and some points are missing due to failure of the strain gauges or rupture of the CFRP wrap. Fig. 6 also reveals that the hoop strains at the corner regions are all smaller than those at the middle regions of cross-sectional side, although the first rupture of CFRP usually appeared at the corner regions. This means that the dilation of concrete at each middle side region was much larger than at the corner regions. The CFRP wrap was unable to effectively confine the concrete dilation at the middle of each side. Consequently, the effective hoop strain (ε_{fe}) at failure should be obtained from averaging the hoop strain gauges located at the corners. The mean measured rupture strain of all the strain gauges around the entire perimeter of confined section overestimates the effective rupture strain of FRP. For FRP-confined RC columns (i.e. R150L1 and R300L2), several strain gauges (i.e. #1 and #2) mounted at the corner regions measured larger values than other corner strain gauges. The reason for such peculiar behavior may be due to the longitudinal reinforcing bars buckling which will increase the hoop strain of the CFRP. It can also be observed that the FRP rupture strain of small columns confined with FRP is generally larger than that in larger FRP-confined columns. Similar results have also been obtained in a previous study by Wang et al. [25].

In conclusion, the distribution of FRP hoop strain is not uniform around the perimeter of confined square columns. The hoop strain at the corner regions is smaller than the middle region of each side. The rupture strain at the corner regions should be the effective rupture strain of FRP. This is because the corner regions contain the effectively confined areas while the middle region of each side is unable to effectively provide confinement. In addition, the effective rupture strain of FRP generally decreases with an increase of column cross-sectional size.

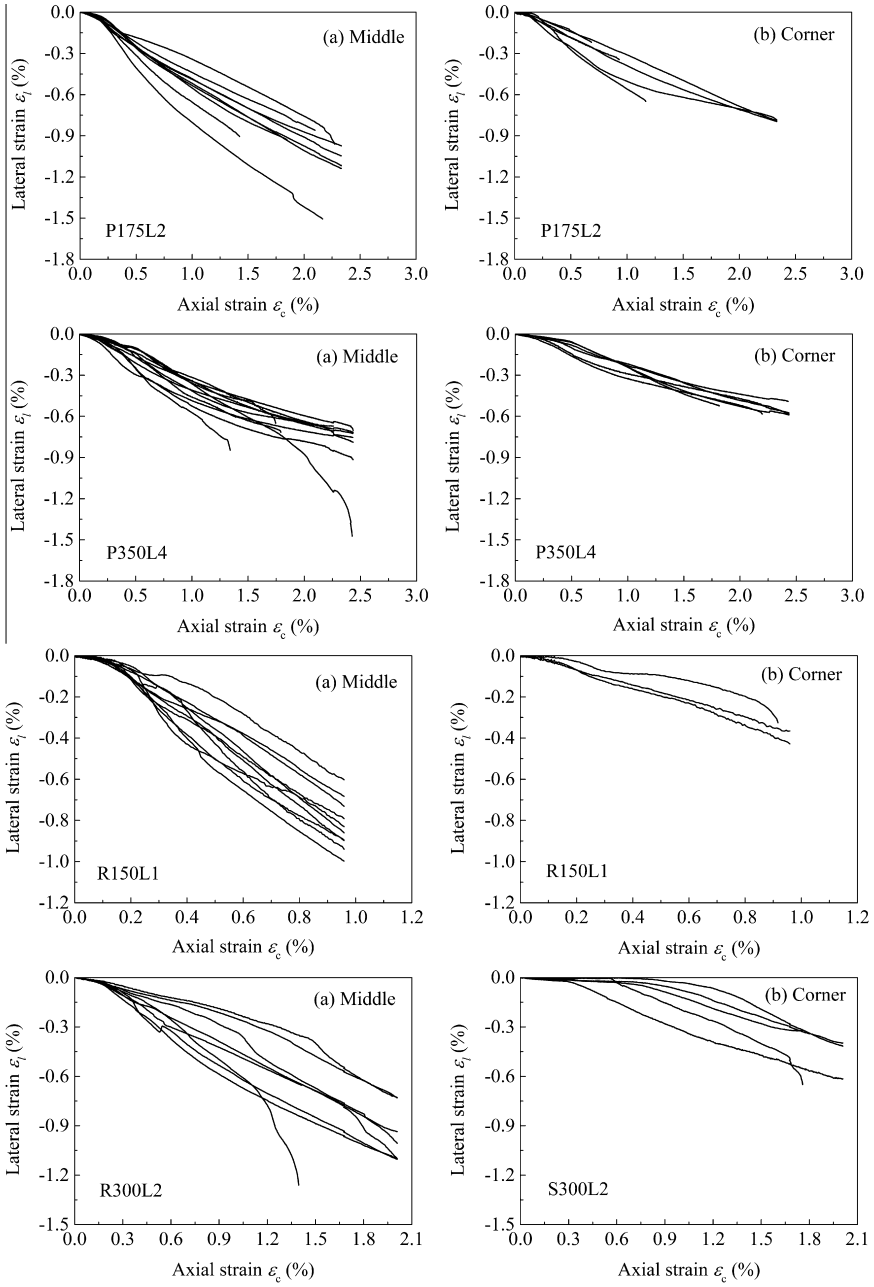

Fig. 6. Hoop strain versus axial stress for selected specimens.

3.4. Effective confinement provided by CFRP wrap

As discussed above, the rupture strain at the corner regions should be defined as the effective lateral rupture strain of FRP. Based on Eq. (1), the lateral confinement of FRP is influenced by the effective lateral rupture strain of FRP. Therefore, the reduction of effective rupture strain of FRP with an increase of column size will result in a decrease of effective lateral confinement. This is the reason that the larger specimens exhibited different axial stress-strain responses compared with small columns with the same theoretical lateral confinement in each group. The effective hoop rupture strain of FRP wrap can be calculated using an equation developed by Pessiki et al. [21] and later adopted by Lam and Teng [6] and ACI 440.2R-08 [14]. The equation is given herein:

$$\varepsilon_{fe} = \kappa_\varepsilon \varepsilon_{fu} \tag{4}$$

where ε_{fe} = effective lateral rupture strain of FRP, κ_ε = efficiency factor, and [ε_{fu} = ultimate tensile strain of FRP derived from flat coupon tests.The efficiency factor is usually constant in existing theoretical lateral FRP confining pressure models and the size effect on the rupture strain of FRP is not considered. Based on the test results provided in Table 1, Fig. 8 shows a strong correlation between the ratio of $\varepsilon_{fe}/\varepsilon_{fu}$ (i.e. Effective strain factor, $\kappa_{\varepsilon)}$ and the normalized cross-sectional size (b/100). By utilizing the test results of this paper and Wang et al.'s [25] study in a regression analysis, the modified effective strain factor of FRP is proposed by the following equation. The correlation coefficient (R^2) is 0.95:

$$\kappa_\varepsilon = \frac{\varepsilon_{fe}}{\varepsilon_{fu}} = 1 - 0.38\left(\frac{b}{100}\right)^{0.41} \qquad 100 \leqslant b \leqslant 400 \tag{5}$$

The model is applicable over the ranges of cross-sectional widths 100 mm to 400 mm. For specimens with cross-sectional

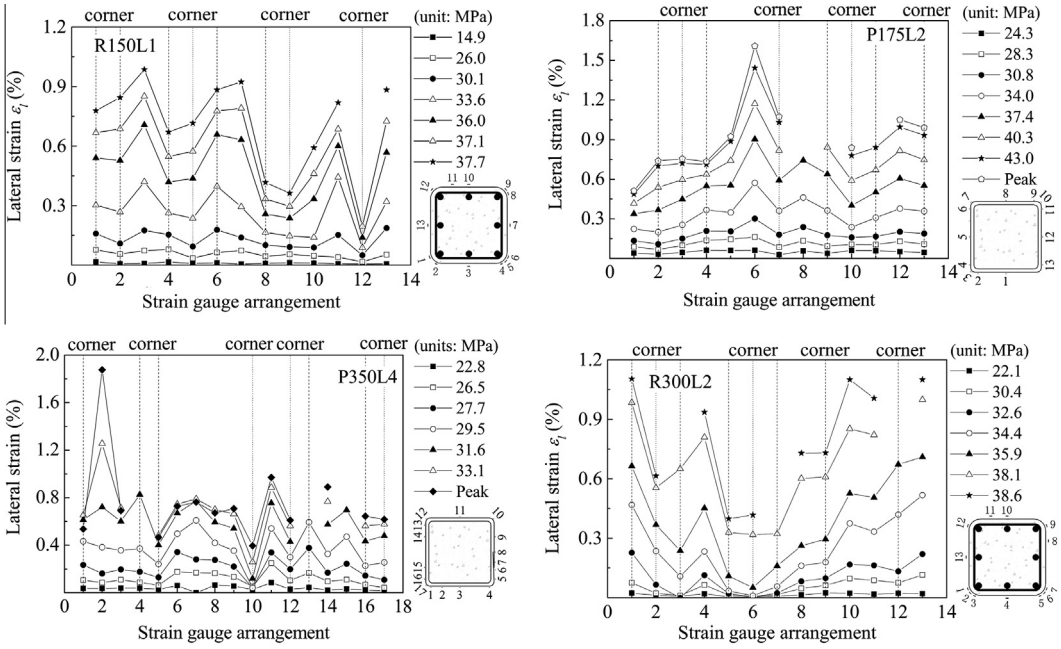

Fig. 7. Typical hoop strain distribution on CFRP wrap.

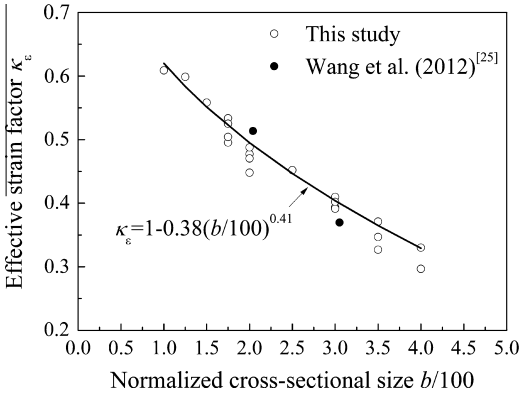

Fig. 8. Effective strain factor versus normalized cross-sectional size.

sizes larger than 400 mm, the factor is suggested equal to that of 400 mm width specimens which is approximately equal to 0.33. However, for columns with widths larger than 400 mm, future experimental investigations are required. It should also be noted that the model was proposed based on the recommended corner radius of 0.15b. Further studies need to be conducted to relate the effective lateral rupture strain of FRP to corner radius. On the basis of the proposed efficiency factor model, the effective lateral confining pressure of FRP wrap considering size effect can then be calculated by incorporating the modified effective strain factor of Eq. (5) into Eq. (1).

3.5. Application of effective strain factor on ultimate stress model proposed by ACI

The test results and discussion in the preceding part of the paper have revealed that the effective confinement of FRP decreases with an increase of cross-sectional size. This results in an ultimate compressive strength decrease with an increase of cross-sectional size for FRP-confined square concrete columns with the same theoretical confinement. To better understand and illustrate the influence of cross-sectional size on the ultimate strength capacity of FRP-confined columns, the proposed effective strain factor is incorporated into the ultimate compressive stress model adopted by ACI 440.2R-08 [14]. The ultimate compressive stress f_{cc} is therefore calculated as follows

$$f_{cc} = f'_c + \psi_f 3.3 \kappa_a f_l \tag{6}$$

where f'_c = unconfined cylinder compressive strength of concrete, ψ_f = additional reduction factor (=0.95), and f_l = effective confinement pressure of FRP calculated from Eq. (1) and with the effective hoop strain of FRP at failure using the model proposed in Eq. (5). The efficiency factor accounting for the geometry of the section, κ_a, is calculated as follows

$$\kappa_a = \left[1 - \frac{2(b - r_c^2)}{3A_g} - \rho_g\right] / (1 - \rho_g) \tag{7}$$

where b = width of the cross section, r_c = corner radius, A_g = gross cross-sectional area, and ρ_g = ratio of longitudinal steel to gross cross-sectional area.

The comparison between test results and predictions of the ultimate compressive stress model before and after size effect modification to the calculation of FRP confining pressure is given in Table 3 and Fig. 9. The strength model proposed in ACI 440.2R-08 [14] is for FRP-confined concrete columns with bilinear ascending stress-strain curves. The size effect on effective lateral confinement is pronounced in FRP-confined larger-sized square columns. Specimens of FRP-confined concrete columns with cross-sectional size larger than 200 mm in this study and in Wang et al.'s [25] study were selected to verify the stress model.

It can be observed from Table 3 and Fig. 9 that the original stress model generally overestimates the axial stress capacity for FRP-confined larger-sized columns. After size-effect modification though, the predictions of ultimate stresses correlate better with the test results. It can be concluded from the application of the modified effective strain factor that the influence of cross-sectional size should be considered when designing FRP retrofitting for larger-sized square columns. In addition, stress-strain models based on the test results of smaller square columns may not be suitable for larger-sized square columns. Furthermore, the size effect on the strength of unconfined concrete also suggested

Table 3
Comparison of test results and predictions of stress models before and after modification.

Specimen		B (mm)	Layers (n)	Ultimate stress f_{cc} (MPa)		
				Test	Original	Modified
This study	P200L1	200	1	27.5	31.7	30.7
	P200L2	200	2	37.6	38.0	36.0
	P300L3	300	3	35.2	38.0	34.1
	P400L4	400	4	26.9	38.0	32.5
	P250L2	250	2	33.4	35.4	33.1
	P300L2	300	2	31.3	33.8	31.2
	P350L2	350	2	26.7	32.6	29.9
	P350L4	350	4	32.9	39.8	34.3
Wang et al. (2012)	S1H1L2M	305	2	30.7	32.5	30.2
	S1H1L2C	305	2	27.9	32.5	30.2
	S1H2L2M	305	2	30.9	32.5	30.2
	S1H1L2D1	305	2	30.1	32.5	30.2
	S1H1L2D2	305	2	30.3	32.5	30.2
	S1H1L3M	305	3	33.3	35.9	32.6
	S1H1L3C	305	3	33.9	35.9	32.6
	S1H2L3M	305	3	35.8	35.9	32.6
	S1H1L3D1	305	3	32.8	35.9	32.6
	S1H1L3D2	305	3	33.9	35.9	32.6
	S2H0L2M	204	2	31.4	36.0	34.3
	S2H0L2P	204	2	27.9	36.0	34.3
	S2H0L2C	204	2	32.1	36.0	34.3

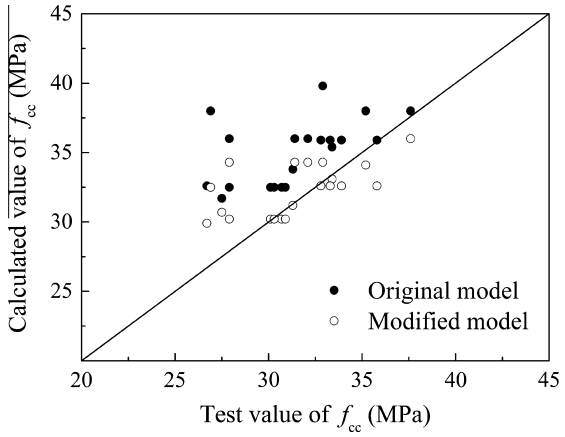

Fig. 9. Comparison between test and predicted ultimate stress.

to be considered by multiply an additional safety reduction factor in the calculated ultimate strength of confined columns.

4. Conclusions

In this paper, 23 CFRP-confined square concrete columns subjected to monotonic axial compressive loading were tested. The purpose of this study was to investigate size effect on the axial stress-strain response of FRP-confined square columns. The following conclusions are able to be drawn from this work:

1. After considering size effect on the unconfined cylinder compressive strength of concrete, specimen size had no obvious effect on the axial stress-strain behaviors of FRP-confined columns with cross-sectional size equal to and less than 300 mm. However, the axial stress-strain response exhibited significant difference with an increase of specimen size, especially for large-scale columns (i.e. cross-section sizes equal to and larger than 350 mm). The actual confinement of FRP was not the same for the larger and small specimens with the same theoretical lateral FRP confinement pressure.
2. The lateral strain at corner regions is smaller than that at the middle region of each side. In addition, the corner strains were observed to decrease with an increase of specimen size. The rupture strain at the corner regions is therefore recommended to be defined as the effective lateral rupture strain of FRP. As a result, the confinement of CFRP decreases with an increase in specimen sizes. Based on the test results, a modified effective strain factor model considering size effect has been proposed for CFRP-confined square columns.
3. The influence of cross-sectional size on the effective rupture strain of FRP should be considered when designing FRP confinement for larger-sized square columns. The stress-strain models proposed based on the test results of smaller square columns currently may overestimate the stress capacity of larger-sized square columns.
4. The conclusions presented in this paper are based on limited experimental data. Additional experimental investigations on the size effect of FRP-confined square and rectangular columns are required in order to better understand the influence of a wide range of geometric and material properties. In addition, research on the influence of corner radius to cross-sectional width ratio on the size effect of confinement provided by FRP is also required.

Acknowledgements

This research was supported by the National Natural Science Foundation of China (Grant Nos. 51478143, 51408153, and 51278150) and the National Key Basic Research Program of China (973 Program, Grant No. 2012CB026200) and also by the Fundamental Research Funds for the Central Universities (Grant No. HIT.NSRIF.2015097).

References

[1] A. Mirmiran, M. Shahawy, M. Samaan, H.E. El-Echary, J.C. Mastrapa, O. Pico, Effect of column parameters on FRP-confined concrete, J. Compos. Constr. 2 (4) (1998) 175–185.
[2] P. Rochette, P. Labossière, Axial testing of rectangular column models confined with composites, J. Compos. Constr. 4 (3) (2000) 129–136.
[3] Y. Xiao, H. Wu, Compressive behavior of concrete confined by carbon fiber composite jackets, J. Mater. Civ. Eng. 12 (2) (2000) 139–146.
[4] L. Lam, J.G. Teng, Design-oriented stress-strain model for FRP-confined concrete, Constr. Build. Mater. 17 (6–7) (2003) 471–489.
[5] L. Lam, J.G. Teng, Design-oriented stress-strain model for FRP-confined concrete in rectangular columns, J. Reinf. Plast. Compos. 22 (13) (2003) 1149–1186.
[6] L. Lam, J.G. Teng, Ultimate condition of fiber reinforced polymer-confined concrete, J. Compos. Constr. 8 (6) (2004) 539–548.
[7] J.G. Teng, T. Jiang, T. Lam, Y.Z. Luo, Refinement of a design-oriented stress-strain model for FRP-confined concrete, J. Compos. Constr. 13 (4) (2009) 269–278.
[8] M.N. Youssef, Stress-Strain Model for Concrete Confined by FRP Composites (Ph.D. thesis), University of California, Irvine, California, USA, 2003.
[9] M.N. Harajli, Axial stress-strain relationship for FRP confined circular and rectangular concrete columns, Cem. Concr. Compos. 28 (10) (2006) 938–948.
[10] R. Eid, P. Paultre, Analytical model for FRP-confined circular reinforced concrete columns, J. Compos. Constr. 12 (5) (2008) 541–552.
[11] Y.F. Wu, L.M. Wang, Unified strength model for square and circular concrete columns confined by external jacket, J. Struct. Eng. 135 (3) (2009) 253–261.
[12] Y.F. Wu, Y.W. Zhou, Unified strength model based on Hoek-Brown failure criterion for circular and square concrete columns confined by FRP, J. Compos. Constr. 14 (2) (2010) 175–184.
[13] S.T. Smith, S.J. Kim, H.W. Zhang, Behavior and effectiveness of FRP wrap in the confinement of large concrete cylinders, J. Compos. Constr. 14 (5) (2010) 573–582.
[14] American Concrete Institute (ACI), Guide for the Design and Construction of Externally Bonded FRP Systems for Strengthening Concrete Structures, 2008. ACI 440.2R-08, Farmington Hills, MI, USA.
[15] Canadian Standard Association (CSA), Design and Construction of Building Components with Fiber-Reinforced Polymers, 2002. CSA-S806-2002, Mississauga, Ontario, Canada.

[16] M. Thériault, K.W. Neale, S. Claude, Fiber-reinforced polymer-confined circular concrete columns: investigation of size and slenderness effects, J. Compos. Constr. 8 (4) (2004) 323–331.
[17] H.M. Elsanadedy, Y.A. Al-Salloum, S.H. Alsayed, R.A. Iqbal, Experimental and numerical investigation of size effects in FRP-wrapped concrete columns, Constr. Build. Mater. 29 (1) (2012) 56–72.
[18] H. Toutanji, M. Han, J. Gilbert, S. Matthys, Behavior of large-scale rectangular columns confined with FRP composites, J. Compos. Constr. 14 (1) (2010) 62–71.
[19] S.A. Carey, K.A. Harries, Axial behavior and modeling of confined small-, medium-, and large-scale circular sections with carbon fiber-reinforced polymer jackets, ACI Struct. J. 102 (4) (2005) 596–604.
[20] Z. Zhu, I. Ahmad, A. Mirmiran, Effect of column parameters on axial compression behavior of concrete-filled FRP tubes, Adv. Struct. Eng. 8 (4) (2005) 443–449.
[21] S. Pessiki, K.A. Harries, J.T. Kestner, R. Sause, J.M. Ricles, Axial behavior of reinforced concrete columns confined with FRP jackets, J. Compos. Constr. 5 (4) (2001) 237–245.
[22] M.J. Masia, T.N. Gale, N.G. Shrive, Size effect in axially loaded square-section concrete prisms strengthened using carbon fiber reinforced polymer wrapping, Can. J. Civ. Eng. 31 (1) (2004) 1–13.
[23] S. Rocca, Experimental and Analytical Evaluation of FRP-Confined Large Size Reinforced Concrete Columns (Ph.D. thesis), University of Missouri-Rolla, Rolla, MO, USA, 2007.
[24] Y.F. Wang, H.L. Wu, Size effect of concrete short columns confined with aramid FRP jackets, J. Compos. Constr. 15 (4) (2011) 535–544.
[25] Z.Y. Wang, D.Y. Wang, S.T. Smith, D.G. Lu, CFRP-confined large square RC columns. I: experimental investigation, J. Compos. Constr. 16 (2) (2012) 150–160.
[26] L.M. Wang, Y.F. Wu, Effect of corner radius on the performance of CFRP-confined square concrete columns: test, Eng. Struct. 30 (2) (2008) 493–505.
[27] American Society for Test and Materials (ASTM), Standard Test Method for Tensile Properties of Polymer Matrix Composite Materials, 2008. ASTM D3039/D3039M-08, West Conshohocken, PA, USA.
[28] American Society for Test and Materials (ASTM), Standard Test Methods for Tension Testing of Metallic Materials, 2008. ASTM E8/E8M, West Conshohocken, PA, USA.
[29] Z.P. Bažant, Size effect in blunt fracture: concrete, rock, metal, J. Eng. Mech. 110 (4) (1984) 518–535.
[30] Z.P. Bažant, Size effect in compression fracture: splitting crack band propagation, J. Eng. Mech. 123 (42) (1997) 162–172.
[31] Z.P. Bažant, Size effect on structural strength: a review, Arch. Appl. Mech. 69 (1999) 703–725.
[32] J.K. Kim, S.T. Yi, C.K. Park, S.H. Eo, Size effect on compressive strength of plain and spirally reinforced concrete cylinders, ACI Struct. J. 96 (1) (1999) 88–94.
[33] H. Zhou, Experimental Study on Size Effect on Concrete Strength (Master thesis), Dalian University of Technology, Dalian, China, 2010 (in Chinese).
[34] B.D. Scott, R. Park, M.J.N. Priestley, Stress-strain behavior of concrete confined by overlapping hoops at low and high strain rates, ACI Struct. J. 79 (1) (1982) 13–27.